PROCEEDINGS OF SPIE

SPIEDigitalLibrary.org/conference-proceedings-of-spie

# An optically-transparent PVDF transducer array for photoacoustic tomography

He Hu, Cheng Fang, Jun Zou

He Hu, Cheng Fang, Jun Zou, "An optically-transparent PVDF transducer array for photoacoustic tomography," Proc. SPIE 11960, Photons Plus Ultrasound: Imaging and Sensing 2022, 119601B (3 March 2022); doi: 10.1117/12.2609268

SPIE.

Event: SPIE BiOS, 2022, San Francisco, California, United States

# An Optically-Transparent PVDF Transducer Array for Photoacoustic Tomography

He Hu, Cheng Fang, Jun Zou
Dept. of Electrical and Computer Engineering, Texas A&M University, College Station, TX, USA 77843-3128

## ABSTRACT

Photoacoustic tomography (PAT) is a hybrid imaging technique, which is capable of providing abundant optical contrast and high spatial resolution at deep penetration depth. One fundamental challenge in current PAT system design is caused by the opaque structure of the ultrasound transducer arrays, which prevents effective light energy delivery onto the imaging target. To address this issue, we report a new optically-transparent PVDF (polyvinylidene fluoride) transducer array for PAT. It consists of a 1D array of 16 elements, each of which has a transparent window to allow the excitation laser pulses to directly pass through. As a result, the optical excitation and ultrasound detection zones are automatically aligned to improve the illumination condition and PA excitation efficiency. Its imaging performance, such as contrast, lateral resolution, and penetration depth has been characterized with optical phantoms. Preliminary ex-vivo PAT experiments on chicken breast tissues have been conducted to demonstrate its imaging capability on real biological samples. The experimental results show that the optically-transparent PVDF transducer array could provide a new solution for the miniaturization and clinical translation of handheld PAT systems.

**Keywords:** Optically-transparent, photoacoustic tomography, PVDF, ultrasound transducer array

## 1. INTRODUCTION

Photoacoustic tomography (PAT) is a hybrid bio-imaging technique, which is capable of providing rich optical contrast and high spatial resolution at a penetration depth well beyond the optical diffraction limit [1-3]. Upon laser pulses illumination, wide-band photoacoustic (PA) waves are induced from the target to be detected by an ultrasound transducer array for image reconstruction. Nevertheless, the optical and acoustic components in current PAT systems are not well compatible with each other, because the opaque structure of the current ultrasound transducer arrays prevents effective light delivery onto the target. To address this issue, the current solution is to route the optical and acoustic beams along different paths. For example, in conventional PAT systems, the opaque ultrasound transducer array is arranged into a circular pattern around the imaging target, while the excitation laser is delivered from the top or the bottom [4-5]. Because of its large footprint, the circular or ring transducer array is mainly suitable for whole-body imaging of small animals on a table top. In the handheld PAT systems, a linear opaque transducer array is sandwiched between two optical fiber bundles positioned at an oblique angle [6]. Nevertheless, this configuration can result in non-uniform illumination, misalignment of optical excitation and ultrasound detection, and a bulky probe structure.

These issues can be addressed by using an optically-transparent ultrasound transducer array to allow the excitation laser pulses to directly pass through, such that the optical excitation and ultrasound detection can be automatically aligned with a compact probe package. Recently, optically-transparent capacitive micromachined ultrasonic transducers (CMUT) [7-9] and optical micromachined ultrasonic transducers (OMUT) [10] arrays have been developed for PAT. However, compared with piezoelectric transducers, CMUTs typically have lower sensitivity, while OMUTs require more complex data acquisition interfaces. More recently, optically-transparent piezoelectric ultrasound transducers have been demonstrated [11-19] which consist of an optically-transparent piezoelectric substrate (e.g., lead magnesium niobate-lead titanate (PMN–PT), lithium niobate ($LiNbO_3$), and polyvinylidene fluoride (PVDF)) sandwiched by two transparent electrodes (e.g., indium tin oxide (ITO)). However, nearly all works published so far are based on a single-element transparent piezoelectric transducer.

This paper reports a new 1-D optically-transparent PVDF transducer array for PAT. Compared with the commonly-used piezoelectric substrates (e.g. lead zirconate titanate (PZT)), PVDF has high optical transparency [16] (in the visible-near infrared (VNIR) range), excellent mechanical flexibility, and good acoustic reception performance [18-19] (e.g., low

Photons Plus Ultrasound: Imaging and Sensing 2022, edited by Alexander A. Oraevsky, Lihong V. Wang
Proc. of SPIE Vol. 11960, 119601B · © 2022 SPIE · 1605-7422 · doi: 10.1117/12.2609268

acoustic impedance, wide acoustic bandwidth, and satisfactory reception efficiency), which make it an ideal candidate for optically-transparent (receiving) transducer arrays. Both the optical and acoustic properties of the PVDF transducer array such as contrast, lateral/axial resolution, and penetration depth are characterized. Preliminary ex-vivo PAT experiments are conducted on chicken breast tissues. The experimental results show that the optically-transparent PVDF transducer array can resolve targets in real biological samples, which provides a new solution for the miniaturization and clinical translation of handheld PAT systems.

## 2. DEVELOPMENT OF TRANSPARENT TRANSDUCER ARRAY

### 2.1 Design and fabrication

The 1-D optically-transparent PVDF transducer array consists of 16 elements (Fig. 1(a)). The width and height of each element are 1 mm and 2 mm, respectively, which also determine the size of each transparent window (Fig. 1(a)). The center-to-center pitch between two neighboring elements is 1.4 mm. The transducer array was fabricated on a single piece of 28-μm-thick PVDF film (Measurement Specialties Inc., Hampton, VA, United States) by the following process flow. Firstly, two shadow masks were laser-cut from a transparency sheet for the deposition of ITO and aluminum electrodes. Secondly, with the two shadow masks, the top side of the PVDF film was firstly coated with a 240-nm-thick ITO layer, followed by the deposition of a 300-nm-thick aluminum layer partly on top of the ITO layer to reduce the contact resistance. Thirdly, the same deposition procedure was repeated on the other side of the PVDF film. For the electrode deposition, shadow mask was visually aligned with the existing electrode patterns. The optical attenuation of the ITO/PVDF/ITO stacked layers is mainly due to the absorption within the films and the reflection at the interfaces. The optical transmittance was measured to be around 60% at the wavelength of 532 nm, which is similar with that obtained previously [18].

After completing the electrode deposition, the transparent PVDF transducer array was fitted onto a curved acrylic sheet with a radius of 40 mm (Fig. 1(b)). 16 multimode optical fibers with a 200-μm core diameter were arranged as an arc array with a laser-cut acrylic spacer to deliver the light onto the target. One end of the optical fibers was bundled together to receive the laser pulses, and the other ends were carefully arranged to conform with each transducer element. Each optical fiber is co-registered and co-centered with one transducer element, which improves the uniformity of the optical illumination. The curved design also enables focused optical illumination and acoustic reception on the target, which improves the strength of the received PA signal.

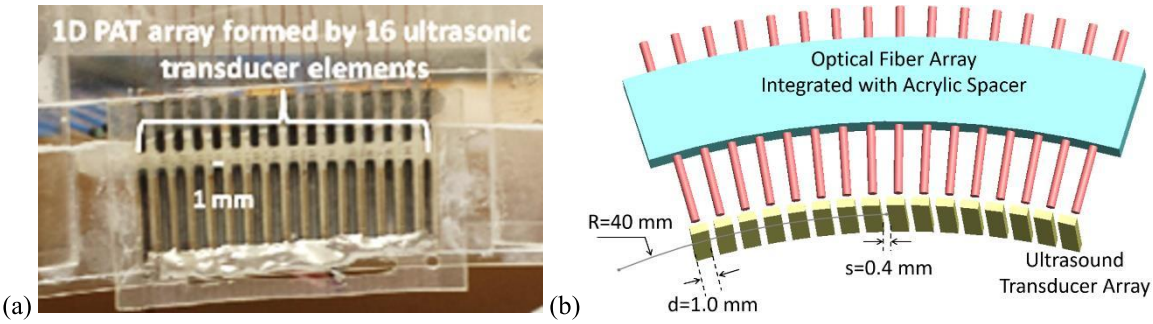


Figure 1. (a) Photo of the optically-transparent PVDF transducer array and (b) diagram of the prototype PA probe head.

### 2.2 PA characterization

The PA performance of the transparent PVDF transducer elements was characterized. Firstly, a piece of cubic agar phantom was prepared as the coupling medium, whose length, width, and thickness were 3 mm, 2 mm, and 2 mm, respectively. Secondly, a piece of black tape was attached to the back side of the agar phantom, and one transducer element was contacted with its front side. Water was applied between the two contacting surfaces to improve the acoustic coupling. Thirdly, 532-nm laser pulses delivered by the corresponding optical fiber were incident onto the black tape through the transparent transducer element and agar phantom for PA excitation. Fig. 2(a) shows a representative PA waveform received by one element of the transducer array after 16 times of averaging, whose frequency spectrum is shown in Fig.

2(b). The measurement results indicate a center frequency of ~4.3 MHz, and a -3dB bandwidth of ~6.5 MHz. The center frequency of the received PA signal is much lower than the theoretical resonance frequency (~25 MHz) of the 28-μm-thick PVDF film, which is mainly due to the diffusive optical illumination onto the black tape.

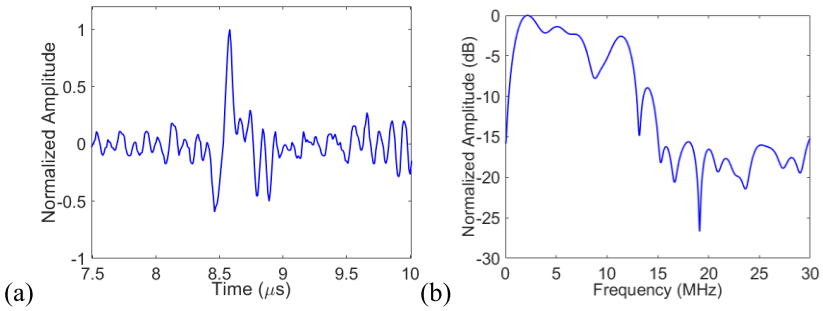


Figure 2. (a) A representative PA waveform received by one transducer element. (b) Acoustic frequency spectrum of the representative PA waveform.

## 3. IMAGING SETUP AND IMAGE RECONSTRUCTION

A PAT setup to characterize the imaging performance of the transparent PVDF transducer array was built (Fig. 3). A Q-switched 532-nm Nd:YAG pulsed laser was used as the light source with pulse repetition rate of 5 Hz and pulse duration around 8 ns. Laser beam was firstly expanded by two lenses and passed through a 100-μm pinhole, and then focused into a bundle of optical fibers to illuminate the targets through the transparent PVDF transducer array. Laser pulse energy was controlled to ensure the laser intensity on target was below the ANSI limit of 20 mJ/cm$^2$. A piece of black tape, serving as the imaging target, was embedded in the agar phantom and chicken breast tissues. A photo detector was used to generate a trigger to synchronize the data acquisition. The 16-channel PA signals were amplified by a preamplifier and captured by a data acquisition (DAQ) card with 16 times average to improve the contrast-to-noise ratio (CNR). The PA image was reconstructed from the 16-channel A-line signals by the synthetic aperture focusing technique (SAFT) based on the Delay-n-Sum algorism [20-22].

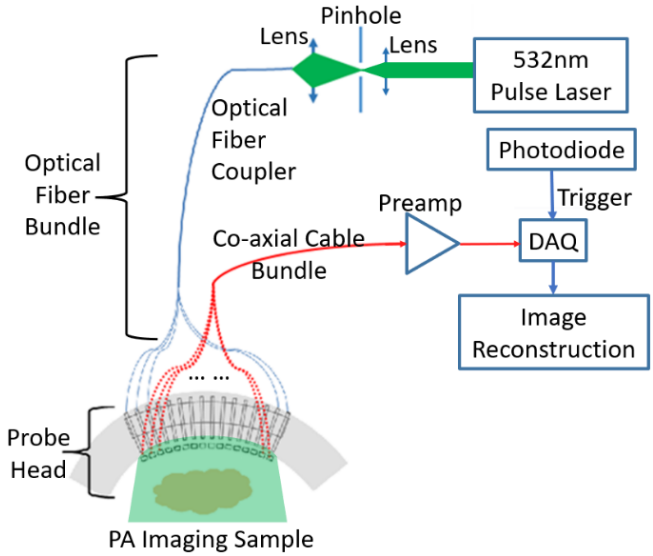


Figure 3. Diagram of the PAT setup based on the 1-D transparent PVDF transducer array.

# 4. PAT EXPERIMENTS AND RESULTS

## 4.1 Lateral and axial resolution

The lateral resolution of the 1-D optically-transparent PVDF transducer array was characterized. Three black-tape strips with widths of 0.5 mm, 1 mm, and 2 mm were fixed at the same depth of 15 mm (where the CNR is maximum) in agar phantom and imaged respectively. As shown in Fig. 4, the black tape with 0.5-mm width could not be resolved and those with 1-mm and 2-mm widths were clearly imaged. This indicates that the lateral resolution is around 1 mm, which is close to the (1-mm) width of the transducer elements. Fig. 5 shows the extracted axial spread profile in the depth direction (along the white dotted line in Fig. 4(b)), where the main peak represents the location of the black-tape target in the reconstructed PA image. The axial resolution is around 0.18 mm determined by the FWHM (full width at half maximum) of the main peak.

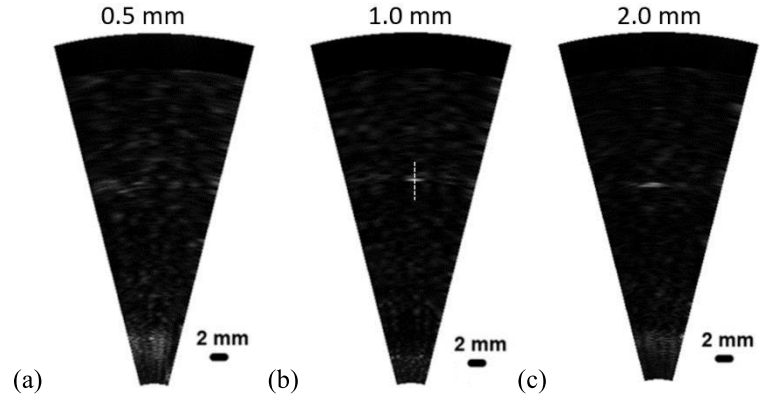


Figure 4. Representative PA images of the black-tape targets with different widths: (a) 0.5 mm; (b) 1.0 mm; (c) 2.0 mm.

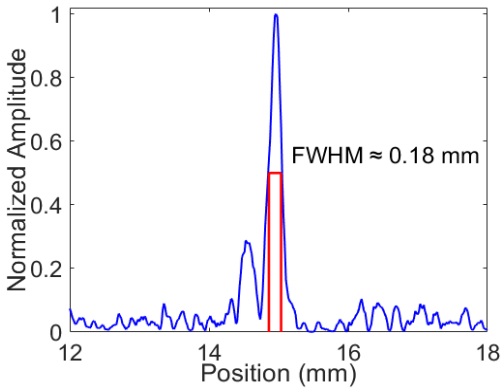


Figure 5. The axial spread profile of the target in image Fig. 4(b), indicating the axial resolution around 0.18 mm.

## 4.2 Ex-vivo imaging

Ex-vivo PAT experiments were conducted on chicken breast tissues (Fig. 6(a)). A piece of 4-mm-wide black tape was embedded in the chicken breast at different depths of 11 mm, 15 mm, and 20 mm. The PA images at depth of 11 mm before and after applying threshold are shown in Figs. 6(b) and 6(c), respectively. PA images at 15-mm and 20-mm depths are not shown because the target is buried into the background noise due to the relatively low CNRs (Table 1). The PA image of the black tape in chicken breast tissue appears to be slightly tilted instead of being perpendicular to the depth axis, possibly due to minor misalignment to the transducer array. In the chicken breast tissue, the CNR consistently decreases with depth, which is mainly due to the strong optical scattering of 532-nm laser in chicken breast tissues.

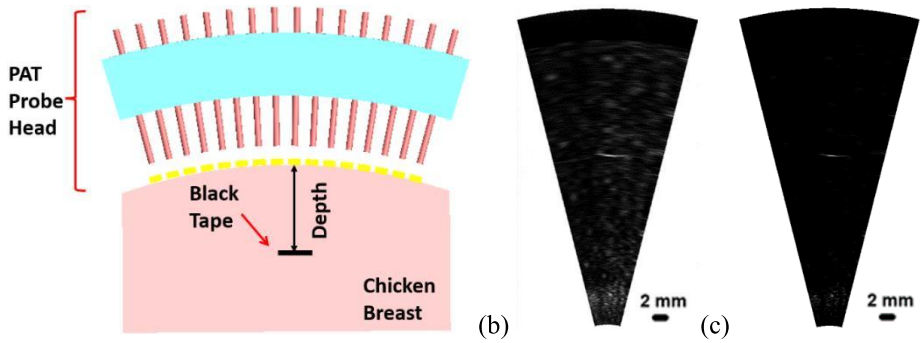


Figure 6. (a) Diagram of the PAT setup to characterize the CNR vs. imaging depth of the 1-D transparent PVDF transducer array with black-tape target in chicken breast. Representative PA images of the black-tape target at depths of 11 mm in chicken breast (b) before and (c) after applying threshold.

Table 1. CNR vs. penetration depth in chicken breast tissues

| Depth in chicken breast tissues (mm) | CNR (dB) |
|---|---|
| 11 | 15.90 |
| 15 | 11.64 |
| 20 | 3.09 |

## 5. CONCLUSIONS

In summary, a new 1-D optically-transparent PVDF transducer array specially designed for PAT has been demonstrated. Its imaging performance in both optical phantoms and biological tissues has been characterized, which shows that a penetration depth around 1 cm can be achieved. By making the transducer array optically transparent, the excitation light can be directly delivered onto the target without any blockage. Such capability could enable simpler and more compact configurations for the miniaturization and clinical translation of handheld PAT systems. In the future, more studies will be conducted to optimize the optical and acoustic performance. Transducer arrays with larger number of elements will be investigated to achieve higher sensitivity and a wider field of view.

## ACKNOWLEDGMENTS

This work was supported in part by an award (CBET-2036134) from the National Science Foundation and a grant (1R01NS115581-01) from the National Institutes of Health to JZ. Any opinions, findings, conclusions, or recommendations presented are those of the authors and do not necessarily reflect the views of the National Science Foundation and the National Institutes of Health.

## REFERENCES

[1] Yao, J. and Wang, L. V., " Photoacoustic tomography: fundamentals, advances and prospects," Contrast media & molecular imaging, 6(5), 332-345 (2011).

[2] Xia, J., Yao, J. and Wang, L. V., "Photoacoustic tomography: principles and advances," Electromagnetic waves (Cambridge, Mass.), 147, 1 (2014).

[3] Wang, L. V. and Yao, J., "A practical guide to photoacoustic tomography in the life sciences," Nature methods, 13(8), 627 (2016).

[4] Lan, H., Jiang, D., Yang, C., Gao, F. and Gao, F., "Real-time photoacoustic tomography system via single data acquisition channel," arXiv preprint arXiv:2001, 07454 (2020).

[5] Jiang, D., Lan, H., Zhong, H., Zhao, Y., Li, H. and Gao, F., "Low-cost photoacoustic tomography system based on multi-channel delay-line module," IEEE Transactions on Circuits and Systems II: Express Briefs, 66(5), 778-782 (2019).

[6] Kim, C., Erpelding, T. N., Jankovic, L., Pashley, M. D. and Wang, L. V., "Deeply penetrating in vivo photoacoustic imaging using a clinical ultrasound array system," Biomedical optics express, 1(1), 278-284 (2010).

[7] Ilkhechi, A. K., Ceroici, C., Dew, E. and Zemp, R., "Transparent capacitive micromachined ultrasound transducer linear arrays for combined realtime optical and ultrasonic imaging," Optics Letters, 46(7), 1542-1545 (2021).

[8] Zhang, X., Wu, X., Adelegan, O. J., Yamaner, F. Y. and Oralkan, Ö., "Backward-mode photoacoustic imaging using illumination through a CMUT with improved transparency," IEEE transactions on ultrasonics, ferroelectrics, and frequency control, 65(1), 85-94 (2017).

[9] Chen, J., Wang, M., Cheng, J. C., Wang, Y. H., Li, P. C. and Cheng, X., "A photoacoustic imager with light illumination through an infrared-transparent silicon CMUT array," IEEE transactions on ultrasonics, ferroelectrics, and frequency control, 59(4), 766-775 (2012).

[10] Zhang, E., Laufer, J. and Beard, P., "Backward-mode multiwavelength photoacoustic scanner using a planar Fabry-Perot polymer film ultrasound sensor for high-resolution three-dimensional imaging of biological tissues," Applied optics, 47(4), 561-577, 2008.

[11] Qiu, C., Wang, B., Zhang, N., Zhang, S., Liu, J., Walker, D., Wang, Y., Tian, H., Shrout, T.R., Xu, Z., Chen, L.Q. and Li, F., "Transparent ferroelectric crystals with ultrahigh piezoelectricity," Nature, 577(7790), 350-354 (2020).

[12] Chen, H., Osman, M., Mirg, S., Agrawal, S., Cai, J., Dangi, A. and Kothapalli, S. R., "Transparent ultrasound transducers for multiscale photoacoustic imaging," Photons Plus Ultrasound: Imaging and Sensing 2021, 11642, 1164220, International Society for Optics and Photonics (2021).

[13] Dangi, A., Agrawal, S. and Kothapalli, S. R., "Lithium niobate-based transparent ultrasound transducers for photoacoustic imaging," Optics letters, 44(21), 5326-5329 (2019).

[14] Brodie, G. W., Qiu, Y., Cochran, S., Spalding, G. C. and Macdonald, M. P., "Optically transparent piezoelectric transducer for ultrasonic particle manipulation," IEEE transactions on ultrasonics, ferroelectrics, and frequency control, 61(3), 389-391 (2014).

[15] Chen, R., He, Y., Shi, J., Yung, C., Hwang, J., Wang, L. V. and Zhou, Q., "Transparent High-Frequency Ultrasonic Transducer for Photoacoustic Microscopy Application," IEEE transactions on ultrasonics, ferroelectrics, and frequency control, 67(9), 1848-1853 (2020).

[16] Blumenröther, E., Melchert, O., Kanngießer, J., Wollweber, M. and Roth, B., "Single Transparent Piezoelectric Detector for Optoacoustic Sensing—Design and Signal Processing," Sensors, 19(9), 2195 (2019).

[17] Niederhauser, J. J., Jaeger, M., Hejazi, M., Keppner, H. and Frenz, M., "Transparent ITO coated PVDF transducer for optoacoustic depth profiling," Optics communications, 253(4-6), 401-406 (2005).

[18] Fang, C., Hu, H. and Zou, J., "A Focused Optically Transparent PVDF Transducer for Photoacoustic Microscopy," IEEE Sensors Journal 20(5), 2313-2319 (2019).

[19] Fang, C. and Zou, J., "Acoustic Resolution Photoacoustic Microscopy (AR-PAM) Based on an Optically Transparent Focused Transducer with a High Numerical Aperture," Optics Letters, 46(13), 3280-3283 (2021).

[20] Karaman, M., Li, P. C. and O'Donnell, M., "Synthetic aperture imaging for small scale systems," IEEE transactions on ultrasonics, ferroelectrics, and frequency control, 42(3), 429-442 (1995).

[21] Doctor, S. R., Hall, T. E. and Reid, L. D., "SAFT—the evolution of a signal processing technology for ultrasonic testing," NDT international, 19(3), 163-167 (1986).

[22] Schickert, M., Krause, M. and Müller, W., "Ultrasonic imaging of concrete elements using reconstruction by synthetic aperture focusing technique," Journal of materials in civil engineering, 15(3), 235-246 (2003).